# Markov Decision Process for Image-Guided Additive Manufacturing

Bing Yao <sup>6</sup>, Farhad Imani <sup>6</sup>, and Hui Yang <sup>6</sup>, Senior Member, IEEE

Abstract—Additive manufacturing (AM) is a process to produce three-dimensional parts with complex and free-form geometries layer by layer from computer-aided-design models. However, realtime quality control is the main challenge that hampers the wide adoption of AM. Advancements in sensing systems facilitate AM monitoring and control. Realizing full potentials of sensing data for AM quality control depends to a great extent on effective analytical methods and tools that will handle complicated imaging data, and extract pertinent information about defect conditions and process dynamics. This letter considers the optimal control problem for AM parts whose layerwise defect states can be monitored using advanced sensing systems. Specifically, we formulate the in situ AM control problem as a Markov decision process and utilize the layerwise imaging data to find an optimal control policy. We take into account the stochastic uncertainty in the variations of layerwise defects and aim at mitigating the defects before they reach the nonrecoverable stage. Finally, the model is used to derive an optimal control policy by utilizing the defect-state signals estimated from layerwise images in a metal AM application.

Index Terms—Additive manufacturing, optimal control policy, Markov decision process, optical imaging, defect mitigation.

### I. INTRODUCTION

ODERN manufacturing industry faces increasing demands to provide highly personalized products and services to gain competitive advantages in the global market. This trend calls for the next-generation manufacturing system that is highly flexible and adaptive to complex and customized designs. For example, additive manufacturing (AM) is a process to produce a 3D part layer by layer from computer-aided design (CAD) models. It enables the creation of complex, freeform geometries that are difficult, if not impossible, to realize using conventional subtractive and formative manufacturing techniques. AM thus overcomes longstanding design and manufacturing constraints. The global market for AM processes and services is expected to rise to about \$50 billion between 2029 and 2031 [1].

However, AM is currently limited in its ability to perform real-time quality control, which poses great challenges for

Manuscript received February 15, 2018; accepted May 15, 2018. Date of publication May 23, 2018; date of current version June 15, 2018. This letter was recommended for publication by Associate Editor H. Hu and Editor Y. Sun upon evaluation of the reviewers' comments. This work was supported in part by the Lockheed Martin and the NSF CAREER grant (CMMI-1617148). The work of H. Yang was supported by Harold and Inge Marcus Career Professorship. (Corresponding author: Hui Yang.)

The authors are with the Complex System Monitoring, Modeling and Control Laboratory, The Pennsylvania State University, University Park, PA 16802 USA (e-mail: bzy111@psu.edu; fxi1@psu.edu; huy25@psu.edu).

Digital Object Identifier 10.1109/LRA.2018.2839973

widespread applications. For example, microstructure and mechanical properties of AM builds are significantly influenced by process variations and uncertain factors (e.g., thermal effects, hatching pattern, scanning velocity, and extraneous noises). This, in turn, causes internal defects that deteriorate the builds strength, residual stress and hardness. As a result, the rejection rate of AM parts is high. At CIMP-3D of Penn State, seven parts are built simultaneously with the same CAD model in a commercial metal AM machine, only two out of which are defect free. There are still technical challenges to realizing high-confidence AM:

- 1) Quality Assurance: The lack of repeatability in key quality attributes, e.g., dimensional accuracy, and functional integrity (e.g., strength, fatigue resistance, hardness, and abrasion resistance) is a major impediment for wider adoption of additive manufacturing.
- 2) Process Monitoring: Currently, quality assurance in AM is largely dependent on post-build inspection. Long inspection procedure ( $\sim 20\%$  of the manufacturing time) results in a low yield and a high cost process. Rapid advancements in sensing technology provide an opportunity to detect the onset of AM defects prior to the completion of AM builds. However, the dearth of in-situ sensing strategies limits the ability to perform online process monitoring and closed-loop control in AM.
- 3) Optimal Control: AM industries are investing in advanced sensing systems to increase information visibility. However, advanced sensing brings big data. Realizing full potentials of sensing data for AM quality control depends to a great extent on the information-processing capabilities. Indeed, optimal control in AM is challenging due to high varieties in the part design, low-volume production (even one-of-a-kind), and the difficulty to estimate incipient defects and take corrective actions on the fly.

Real-time sensing and process monitoring are critical to quality assurance in AM systems. Due to the high-level complexity of AM process, advanced sensing systems are increasingly developed and implemented to monitor and control the variations in the process of AM build [2], [3]. Advanced sensing provides an unprecedented opportunity to cope with the process complexity and enable on-the-fly quality control of AM processes. Recent advances in communication and electronics have improved the design and development of low-cost and miniaturized sensors for use in AM settings that are previously not possible. In the state of the art, a variety of in-situ sensors (e.g., temperature, vibration, infrared sensors, and video imaging) have been used to capture multi-facet information for

AM process monitoring and control. Notably, the CIMP-3D at the Penn State developed an optical layer-wise imaging technique to monitor the laser powder-bed-fusion AM process. A 36.3-megapixel digital single-lens reflex camera (DSLR) along with multiple flash-lamps are customized and placed inside the chamber of an AM machine to capture the layer-by-layer powder bed images. We have collected large amounts of layerwise imaging data in the fabrication process of AM builds, which are critical to quality inspection and process improvement. However, very little has been done to develop enabling tools that will handle large amount of imaging data, extract pertinent information about defect conditions and process dynamics, and further exploit the acquired knowledge for process monitoring and control.

This letter presents a novel continuous-state mathematical model that leverages the layerwise image data to estimate the state of defect conditions in each layer of AM build, predict the future evolution of defect conditions from one layer to the next, and then model stochastic dynamics of layer-to-layer defect conditions as a Markov process for the derivation of optimal control policy. This investigation aims to develop smart AM through in-situ monitoring of incipient defects and online closed-loop control of part quality and functional integrity. Specifically, corrective actions are executed to counteract and repair incipient defects in AM prior to completion of the build. The evolution of process defects will be detected and mitigated long before they reach the non-recoverable stage.

First, we present the multifractal analysis of layerwise images for characterization and detection of defects in each layer of the AM build [4], [5]. Multifractal analysis captures irregular and nonhomogeneous patterns in multiple scales of AM images. The multifractal spectrum (i.e., a vector of features) is extracted to estimate the defect conditions for each layer. Then, we compute a composite index - Hotelling  $T^2$  statistic - to represent the defect state of each layer in the AM build, which simultaneously consider multi-dimensional variations among these features of multifractal spectrum. As a result, the layer-wise structure of AM build leads to a series of defect states in the form of stochastic signals. Second, we model the defect signals as a real-time, continuous-state stochastic process, which helps to capture the useful information about AM process dynamics that cannot be deciphered otherwise. We leverage the readilyavailable image profiles for each layer to update the predictive distribution of defect signals. In AM process, each layer may affect the next layer and, through that, all subsequent layers. As such, we formulate the AM optimal control as a sequential decision-making problem through the Markov decision process (MDP) framework. Finally, the model is used to derive an optimal control policy by utilizing the defect-state signals estimated from layerwise images in a metal AM application.

This letter addresses the complex structure in the stream of layerwise images for in-situ monitoring and control of nonlinear and nonstationary process in AM, which enables real-time defect mitigation. In-situ quality control of AM processes is conducive to the minimization of layer delamination during manufacturing and warping of the final product; as well as the maximization of final part strength and fatigue resistance.

The remainder of this letter is organized as follows: Section II introduces research background of quality inspection in AM processes. Section III presents the research methodology that integrates in-situ image monitoring with online closed-loop control for smart AM. Case study and experimental results are provided in Section IV. Section V discusses and concludes the present research.

#### II. RESEARCH BACKGROUND

Despite enormous progress in recent years, quality assurance in AM remains an enduring challenge [6]. Currently, quality assurance in AM is largely limited to offline data-driven techniques and traditional optimization approaches (e.g., design of experiments). For example, Huang et al. [7] developed prescriptive modeling approaches to predict the deformation of 2D and 3D shapes [8], [9]. Further, optimal compensation is implemented in the CAD model to increase the geometric accuracy in the final AM build. Also, existing geometric dimensioning and tolerancing (GD&T), and surface metrology techniques, which are primarily offline and intended for regular Euclidean features, are not amenable for assessment of AM parts with complex free-form geometries [10]. In the absence of quantitative approaches for assessing surface morphology and dimensional fidelity, benchmarking of AM builds remains relegated to qualitative attributes [11].

Although sensor-based monitoring of AM has been introduced [2], [12], these data-driven approaches mainly focus on defect identification and do not suggest online corrective actions. Sensor-based monitoring of AM processes is among the highest priorities for realizing the high-confidence AM technologies. Infrared camera has been proposed to capture the thermal distribution of AM parts, and provide information on residual stress and microstructures of 3D products. Krauss et al. [13] detected material discontinuities and process deviations by monitoring the temperature distribution of AM layers using an infrared camera in the selective laser melting (SLM) process. Rodriguez et al. [14] developed the in-situ thermography to identify absolute thermal non-uniformity in layer surfaces of AM parts for quality control. High-resolution cameras with visible wavelength also play an important role in monitoring and detection of defects in AM layers so as to detect process errors and material discontinuities. Grasso et al. [15] localized defects using a highspeed camera (i.e., an Olympus I-speed 3 camera) for in-situ monitoring of SLM processes. The CIMP-3D at the Penn State developed an in-chamber imaging system with high-definition 36.3 megapixel DSLR 164 AQ4 camera (Nikon D800E) with multiple flash modules [16]. We collected in-situ images of layerwise finishes of AM builds both after laser exposure and after recoating.

However, in-situ imaging systems bring large amounts of complex structured image data that call upon the development of new image-based statistical process control (SPC) methods. Existing SPC methods mainly focus on key product characteristics, linear and nonlinear profiles, as opposed to image profiles that are nonlinear and nonstationary. In the past few years, in-situ image data have attracted increasing interests. For example, Du

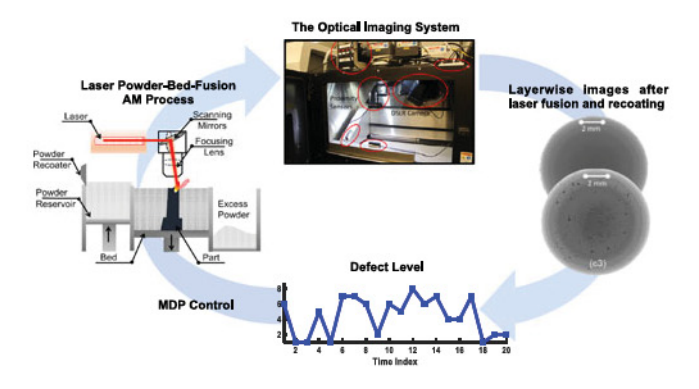


Fig. 1. Flow diagram of the research methodology.

et al. analyzed hyperspectral images of poultry carcasses [17]. A spectral band selection approach was developed to extract features for the detection of skin tumors. Kan et al. developed a novel dynamic network methodology for monitoring and control of high-dimensional imaging streams [18], which is used for monitoring of living cells during the biomanfacturing synthesis process of bio-products [19]. Park et al. investigated microscopic images of nanoparticle dynamics [20]. Morphology of nanoparticles was characterized by a multistage procedure and then semi-automatically classify them into homogeneous groups. Yan et al. proposed to integrate low-rank tensor decomposition with multivariate control charts for image-based process monitoring [21]. In addition, Zhang et al. measured the variations of wafer thickness from image profiles using an adaptive Gaussian process model [22]. Nonetheless, very little has been done to investigate closed-loop control using datadriven models and sequential decision-making strategies. The ability to mitigate incipient defects is critical for AM industries mandating stringent product aesthetics and functional integrity standards.

#### III. RESEARCH METHODOLOGY

In this section, we propose a framework of Markov decision process (MDP) to sequentially control the AM processes. As shown in Fig. 1, the proposed methodology invokes a novel framework for quality assurance in AM by interlinking the following aspects: in-situ imaging measurements → real-time estimation of defect states in layerwise AM images → layer-by-layer optimal control actions → high-confidence quality and functional integrity of AM products. Image-based process monitoring and control is the next vertical step to mitigate scrap and reduce rework rates, and further ensure the economic viability of AM.

#### A. Sensor-Based Modeling of AM Defects

Rapid advances in sensing technology, especially in imaging sensing, facilitate the realization of real-time quality control and defect mitigation in AM processes. For example, the high-speed infrared thermography [23] is used to obtain thermal images for microstructure prediction by determining the grain size resulting from melt pool characteristics. The Center for Innovative Material Processing through Direct Digital Deposition

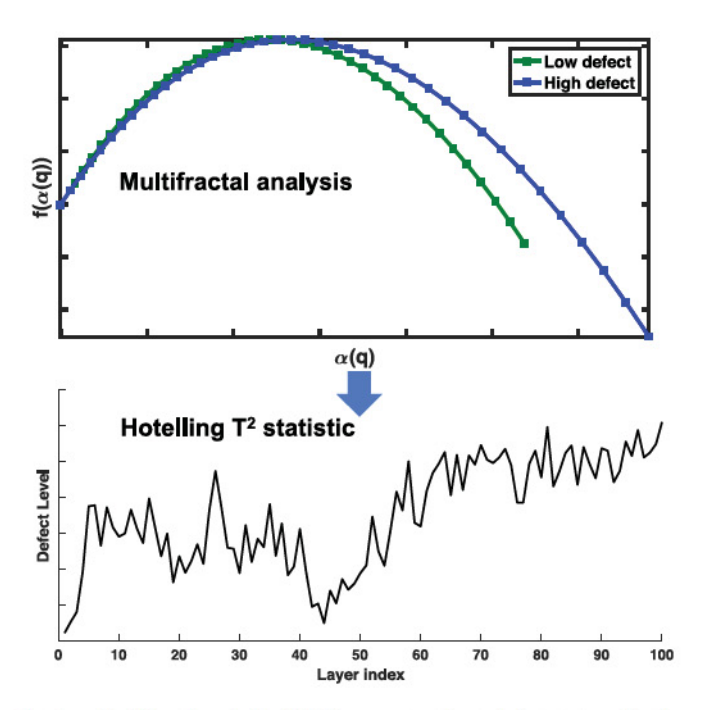


Fig. 2. Multifractal analysis of AM images to estimate defect state and further extract the composite defect index.

(CIMP-3D) at the Pennsylvania State University has developed an optical layer-wise imaging system to monitor the powder-bed-fusion AM process using a consumer-grade 36.3 megapixel DSLR camera [16], [24] as shown in the camera system in Fig. 1. Imaging sensing systems capture the layer-wise defect dynamics of AM process in the form of 2D image profiles. The AM layers are rough, irregular and show fractal pattern under high-resolution cameras. Our previous studies leveraged multi-fractal theory to investigate nonlinear patterns in image profiles for layerwise defect estimation [4], [5].

Note that multifractal analysis extracts a spectrum of singularity exponents to describe the complex scaling behavior of AM images. The local densities of the fractal set are quantified by estimating the mass probability in the  $i^{th}$  box of the image as  $P_i(a) = N_i(a)/N$ , where  $N_i(a)$  denotes the number of pixels in box i of size a, and N is number of the total pixels of the image. Let  $\mu_i(q,a)$  denote the  $q^{th}$  moments of mass probability  $P_i(a)$ , i.e.,  $\mu_i(q,a) = P_i^q(a)/\sum_{i=1}^{N(a)} P_i^q(a)$ . Then, the multifractal spectrum  $f(\alpha(q))$  is computed as:

$$f(\alpha(q)) = \lim_{a \to 0} \frac{\sum_{i=1}^{N(a)} \mu_i(q, a) \ln(\mu_i(q, a))}{\ln a}$$
 (1)

where

$$\alpha(q) = \lim_{a \to 0} \frac{\sum_{i=1}^{N(a)} \mu_i(q, a) \ln(P_i^q(a))}{\ln a}$$
 (2)

Here,  $f(\alpha(q))$  versus  $\alpha(q)$  provides the multifractal spectrum of image profiles. See more details of multifractal analysis of AM imaging profiles in [5]. Fig. 2 (top) shows the multifractal spectra of the AM images shown in Fig. 1.

We further derive the composite index to represent the defect state of each layer by extracting the Hotelling  $T^2$  statistic

from the multifractal spectrum. The Hotelling  $T^2$  statistic are shown to effectively characterize various types of defects in each AM layer [5]. Specifically, let  $F_{T \times k} = [f_1, f_2, \ldots, f_T]'$ , where  $f_t = [f(q_1), f(q_2), \ldots, f(q_k)]'$  denoting the spectrum values from multifractal analysis of layer t. Then, the Hotelling  $T^2$  for a layer indexed with t is

$$T_t^2 = (f_t - \bar{f})^T \Sigma_f^{-1} (f_t - \bar{f})$$
 (3)

where  $\bar{f}$  denotes the sample mean of the multifractal spectra, and  $\Sigma$  is the sample covariance. Thus, the defect composite index for layer t is defined as  $s_t = T_t^2$ , as illustrated in Fig. 2 (bottom).  $s_t$  will be further used to develop an MDP framework for the sequential optimal control of AM processes.

# B. MDP Modeling of AM Processes

Each layer of AM builds is captured by the sensors (i.e., high-resolution cameras) as imaging profile. Hybrid AM machines provide an opportunity to take corrective actions on the fly. Example actions include cutting off a layer, re-fusion, or process adjustments. The corrective action may affect the next layer and, through that, all subsequent layers. The MDP has been widely used in optimal maintenance of engineering systems [25] and cancer screening [26]. However, very little has been done to develop sequential decision-making models for smart AM control through an MDP framework.

Our MDP framework aims to determine whether to instantaneously perform a corrective action (which is denoted as  $a_c$ ) at the cost  $c_a$ , or wait (which is denoted as  $a_w$ ) and continue observing till the next layer with the risk to fail the whole part, i.e., the defect index exceeding the failure threshold. The failure cost is denoted as  $c_f$ , which is set to be bigger than the cost of corrective action  $c_a$ . Note that the observation cost (i.e., the cost of action  $a_w$ ) is generally very small if the sensing system is already in place.

The state space of our MDP model is represented by  $S=(T,\mathcal{R}^+)$ , where  $T=\{1,2,\ldots,T\}$  denotes the set of layer index, and  $\mathcal{R}^+$  is the set of positive real number denoting the set of defect index  $s_t$  (i.e., the  $T^2$  statistic). Let  $P_t^A(s_{t+1}|s_t)$  be the transition probability from state  $s_t$  of layer t to state  $s_{t+1}$  of layer t+1 under the action A, where  $A\in\{a_c,a_w\}$ . Let value function  $V_t(s_t)$  denote the optimal expected total future cost starting in state  $(t,s_t)\in S$ . Then, the optimality equation for the value function is expressed as

$$V_t(s_t) = \begin{cases} c_f & \text{if } s_t > \zeta \\ \min_{A \in \{a_c, a_w\}} \{c_A + \\ \lambda \sum_{s_{t+1}} P_t^A(s_{t+1}|s_t) V_{t+1}(s_{t+1}) \} & \text{if } s_t \leq \zeta \end{cases}$$

where  $\zeta$  is a predefined failure threshold and  $\lambda$  is the discount factor. The definition of the value function  $V_t(s_t)$  follows from the logic that if the defect index  $s_t$  is beyond the failure threshold  $\zeta$ , a high failure cost  $c_f$  is incurred; otherwise, we can either choose to do corrective action  $a_c$  or wait  $a_w$  till the next layer, which is determined based on the expected cost of each action. We will detail how to obtain the optimal policy from our MDP framework in the next subsections.

# C. Structural Property of the Optimal Policy

In this subsection, we will prove that a control limit policy exists for the AM process and show the structural property of the proposed MDP framework. In other words, the AM process is optimal to keep operating (i.e., take action  $a_w$ ) if the defect index  $s_t$  is below a certain control limit  $s_t^*$ , i.e.,  $s_t \leq s_t^*$ , whereas it is optimal to take corrective action  $a_c$  if the defect index  $s_t$  is beyond  $s_t^*$ , i.e.,  $s_t \geq s_t^*$ .

Theorem 1: For each decision epoch, i.e., layer index  $t \in T$ , there exists an optimal control limit  $s_t^* \leq \zeta$ , which means that corrective action (i.e.,  $a_c$ ) needs to be conducted if the defect level  $s_t \geq s_t^*$ , i.e.,

$$A(s_t) = \begin{cases} a_c & \text{if } s_t \ge s_t^* \\ a_w & \text{if } s_t < s_t^* \end{cases}$$
 (4)

*Proof:* If a control limit  $s_t^*$  is obtained for a state  $(t, s_t)$ , taking corrective action  $a_c$  is less expensive than continuing to observe. Hence, the following inequality holds according to the definition of value function  $V_t(s_t)$  in (4):

$$c_a + \lambda E^{a_c}(V_{t+1}(s_{t+1})) \le \lambda E^{a_w}(V_{t+1}(s_{t+1}))$$
 (5)

where  $E^A(\cdot)$  denote the expectation function under the action A. After taking corrective action  $a_c$ , it is expected that the defect level of the next layer (i.e.,  $s_{t+1}$ ) will not be higher than that of the action threshold  $s_t^*$ , i.e.,

$$P_t^{a_c}(s_{t+1} = s, s > s^*|s_t) \ll P_t^{a_c}(s_{t+1} = s, s < s^*|s_t)$$
 (6)

Thus, the left-hand-side (LHS) of (5) satisfies:

$$c_a + \lambda E^{a_c}(V_{t+1}(s_{t+1})) \le c_a + \lambda V_{t+1}(s_t^*)$$
 (7)

In other words, the LHS of (5) is bounded by the right-hand-side (RHS) of (7), which is independent of the random variable of defect index  $s_t$ .

Furthermore, the value function  $V_t(s_t)$  is generally convex and nondecreasing in  $s_t$  for all t. This is due to the fact that if the defect index  $s_t$  is higher, the cost  $V_t(s_t)$  of such state is expected to be bigger. In addition,  $V_t(s_t)$  represents the expected cumulative future cost starting in state of  $(t, s_t)$ . In other words,  $V_t(s_t)$  is nondecreasing in  $s_t$  for all t. Thus, we have the following result

$$E^{a_w}(V_{t+1}(s_{t+1})) \ge V_{t+1}(E^{a_w}(s_{t+1})) \ge V_{t+1}(s_t)$$
 (8)

The second inequality in (8) is due to the fact that when no corrective action is taken (i.e., under the action of  $a_w$ ) for layer t, the distribution of transition probability from state  $s_t$  to state  $s_{t+1}$  is generally left skewed, which means:

$$\int_0^\infty P_t^{a_w}(s_{t+1} = s|s_t)sds \ge s_t \tag{9}$$

which indicates that layer t+1 tends to have higher defect level than current layer t if no corrective action is performed, i.e.,  $E^{a_w}(s_{t+1}) \geq s_t$ .

Equation (8) suggests that the RHS of (5) is nondecreasing in  $s_t$ . Thus, (5) holds for any state  $(t, s_t) \in S$  such that  $s_t \geq s_t^*$ . In other words, the optimal policy for state  $(t, s_t)$  is to take corrective action as long as  $s_t \geq s_t^*$ . In the next section, we will

describe the algorithm to solve our MDP control model based on the structural property.

#### D. Value Iteration to Solve the Optimal Policy

Given the structural property introduced in Section III-C, we develop an efficient value iteration algorithm to solve for the optimal control policy. We first discretize the set of possible defect index into different defect levels as

$$D = \{h, 2h, \dots, \zeta - h, \zeta\} \tag{10}$$

where  $h = \zeta/m$  and m is the cardinality of the discretized space of defect levels D. We denote the defect level at layer index t as  $d_t$ . The discretized state space is then denoted as  $\mathscr{D} =$ (T,D) and  $(t,d_t) \in \mathcal{D}$ . The transition probability matrix for the discretized state space under the action a is computed as follows:

$$P_t^a(d_{t+1}|d_t) = \int_{d_{t+1}-h}^{d_{t+1}} P_t^a(s|d_t)ds \tag{11}$$

Hence, the transition probability under the control policy l at layer index t is computed as

$$P_t^l(d_{t+1}|d_t) = \begin{cases} P_t^{a_c}(d_{t+1}|d_t) & \text{if } d_t \ge l\\ P_t^{a_w}(d_{t+1}|d_t) & \text{if } d_t < l \end{cases}$$
(12)

The corresponding immediate cost function is defined as:

$$c_l = \begin{cases} c_a & \text{if } d_t \ge l \\ 0 & \text{if } d_t < l \end{cases}$$
 (13)

Our goal is to determine the optimal control policy using the value iteration algorithm:

$$\pi^* = \{l_1^*, l_2^*, \dots, l_T^*\} \tag{14}$$

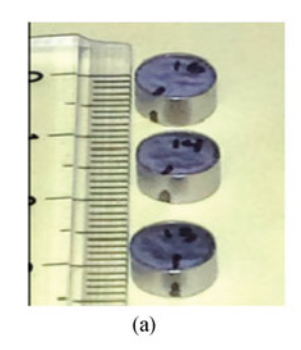
Let n denote the iteration count, and  $V_t^n(d_t)$  denote the value function of state  $(t, d_t)$  at iteration n. The value iteration algorithm consists of the following steps:

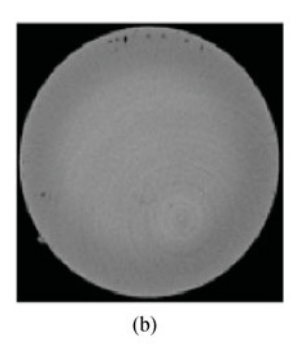
- Step 1: Set  $\lambda$ , n=0 and  $V_t^n(d_t)=0$ ,  $\forall (t,d_t)\in\mathscr{D}$
- Step 2: For each state in the discretized state space S, update the value function using:

$$V_t^{n+1}(d_t)=$$
 
$$\begin{cases} c_f & \text{if } d_t>\zeta \\ \min_{l\in D}\{c_l+\ \lambda\sum_{d_{t+1}}P_t^l(d_{t+1}|d_t)V_{t+1}^n(d_{t+1})\} & \text{if } d_t\leq\zeta \end{cases}$$

- Step 3: Set  $n \leftarrow n+1$
- Step 4: Repeat Step 2 and 3 until  $|V_t^{n+1}(d_t) V_t^n(d_t)| \le$  $\epsilon$ , where parameter  $\epsilon$  is a predefined threshold for convergence and set  $V_t^*(d_t) = V_t^n(d_t), \forall (t, d_t) \in \mathscr{D}$ .
- Return the optimal policy  $\pi^*$  by solving

$$\pi_t^* = \arg\min_{l \in D} \left\{ c_l + \lambda \sum_{d_{t+1}} P_t^l(d_{t+1}|d_t) V_{t+1}^*(d_{t+1}) \right\}$$
(15)





(a) The AM build; (b) 2D image of AM layers.

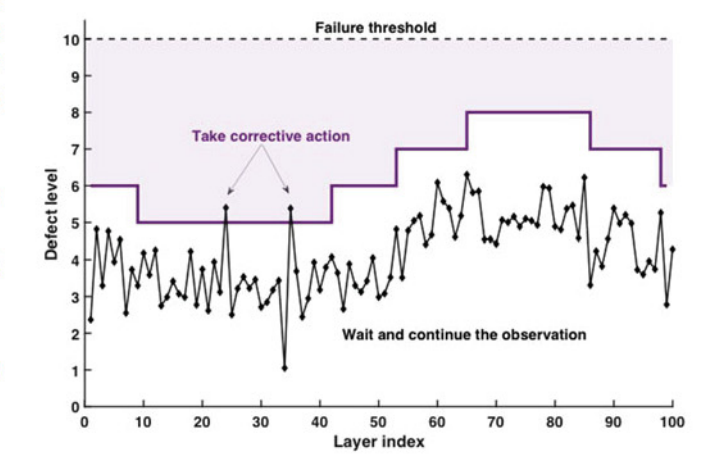
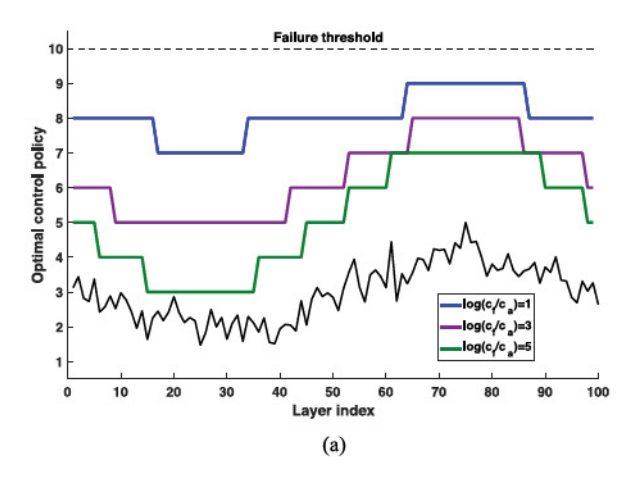


Fig. 4. An illustration of the optimal control policy.

# IV. CASE STUDY

In this section, we implement the proposed MDP framework to solve for the optimal control policy for AM processes. The imaging data in this case study are acquired from a powderbed-fusion AM build as shown in Fig. 3(a). This AM build is fabricated in a direct metal laser sintering (DMLS) process, which is carried out in the EOS M280 system. The layerwise 2D image profiles of the build are collected as shown in Fig. 3(b). Each AM image contains  $7360 \times 4912$  pixels with a pixel size of 12.22  $\mu$ m.

The multifractal analysis is first implemented to analyze the AM images, and compute the composite index, i.e., Hotelling T-square statistic, to represent the defect level of AM layers. The multifractal analysis produces a series of defect states in the form of stochastic signals. We then discretized the continuous defectstate signals into ten states, with  $D = d_1, d_2, \dots, d_{10}$ . We use  $1, 2, \ldots$ , and 10 to denote the defect level  $d_1, d_2, \ldots$ , and  $d_{10}$  in the Figs. 4 and 5. Note that the defect level  $d_{10}$  denotes the failure threshold. We then solve for the optimal control policy using the value iteration algorithm described in Section III-D. Fig. 4 shows an illustration of the obtained optimal policy and how it relates to the defect levels. Note that the purple stepped curve represents the optimal control policy for different layers. If the defect level  $d_t$  exceeds the control threshold, corrective action needs to be conducted to repair the defective layer. Otherwise, the AM process continues operating and the optimal policy is to continue observing.



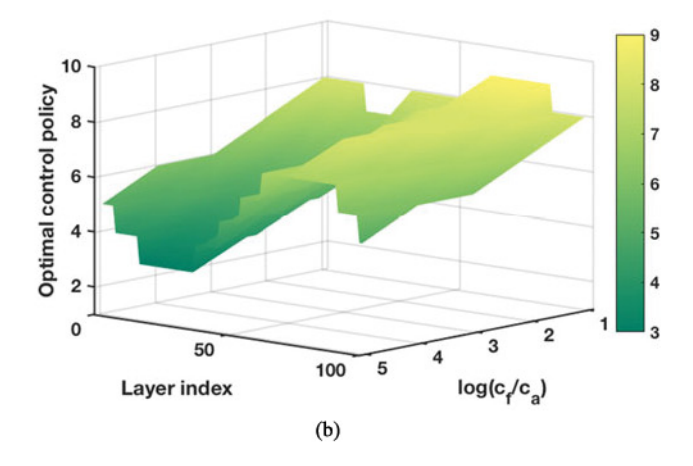


Fig. 5. (a) The variation of optimal control policy with respect to the cost ratio  $c_f/c_a$ ; (b) Surface of the optimal control policy.

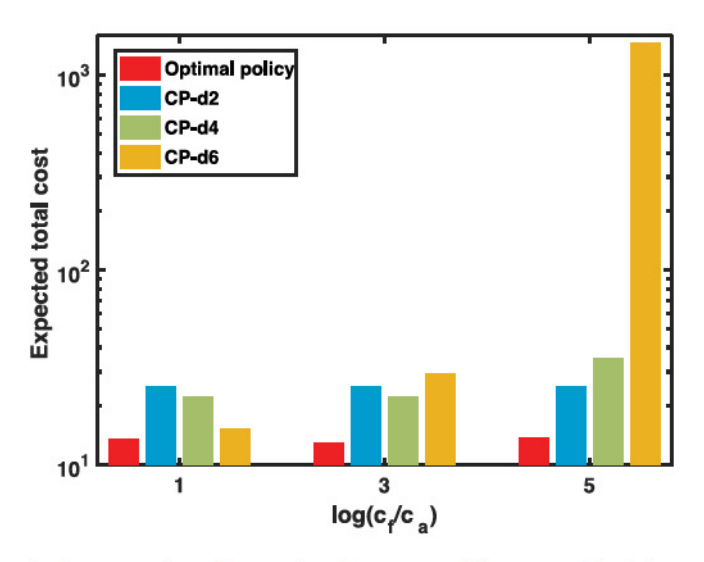


Fig. 6. Comparison of expected total cost among different control policies.

Fig. 5(a) shows the variation of optimal control policy with respect to ratio of the failure  $\cot c_f$  over the  $\cot c_f$  or corrective action  $c_a$ . Fig. 5(b) shows the surface of the optimal control policy with respect to layer index and the  $\cot c_f$  is close to the  $\cot c_f/c_a$  is small (i.e., the failure  $\cot c_f$  is close to the  $\cot c_f$  corrective action), the resulted control policy is closer to the failure threshold as shown by the blue curve in Fig. 5(a), which means the optimal policy is more tolerant of the sudden failure of the AM build. On the other hand, if the  $\cot c_f/c_a$  is large (i.e., significant loss will be incurred if the AM build fails suddenly during the process), the corresponding control policy becomes lower as shown by the green curve, which means the optimal policy is much more conservative in this situation.

To further evaluate the performance of our proposed framework, we compare the expected total cost of the optimal policy derived from our algorithm with three constant policies (CP), i.e., CP-d2, CP-d4, and CP-d6, as shown in Fig. 6. Note that CP-d2 denotes a control policy that whenever the defect signal is higher than the defect level  $d_2$ , corrective action  $a_c$  needs

to be conducted. According Fig. 6, the optimal policy derived from the proposed MDP framework yields the smallest expected total cost under different cost ratios. It is also worth noting that when the cost ratio  $c_f/c_a$  becomes large (i.e., significant loss will be incurred if the AM part fails during the 3D printing process), the expected total cost of the constant policy with a high threshold (e.g., CP-d6) becomes very high. This is due to the fact that if corrective action is conducted only when the defect signal is beyond some high value, the AM part has much greater chance to break down before the completion of the whole process, which leads to a much higher expected total cost.

# V. CONCLUSIONS

Although current AM machines have been greatly improved from early versions, many of the defect problems identified by early researchers in the 1980s (porosity, balling, cracking, thermal management issues, and material issues) persist. High-confidence AM calls upon the development of in-process monitoring and closed-loop control algorithms for optimal management of AM machine operations. Fortunately, rapid advancements in sensing technology, especially in imaging sensing systems, bring large amount of image data and facilitate the realization of in-situ quality control of AM builds.

In this letter, we formulate the optimal control of AM as a sequential decision-making problem through the MDP framework. We first characterize the defect level of layer-wise AM images by capturing the irregular and nonhomogeneous patterns using the multifractal analysis. Second, we compute a composite index to represent the defect level of each layer by extracting the Hotelling  $T^2$  statistic from the multifractal spectrum. Third, we model stochastic dynamics of layer-to-layer defect conditions as a Markov process to determine an optimal control policy. The MDP model is further utilized to solve for the optimal control policy using the defect-state signals estimated from the AM images. Experimental results show that the proposed insitu monitoring and control framework has great potentials for on-the-fly assessment of AM build quality and real-time defect mitigation.

#### REFERENCES

- D. Thomas, "Costs, benefits, and adoption of additive manufacturing: a supply chain perspective," *Int. J. Adv. Manuf. Technol.*, vol. 85, no. 5–8, pp. 1857–1876, 2016.
- [2] S. Berumen, F. Bechmann, S. Lindner, J.-P. Kruth, and T. Craeghs, "Quality control of laser-and powder bed-based additive manufacturing (AM) technologies," *Phys. Procedia*, vol. 5, pp. 617–622, 2010.
- [3] G. Tapia and A. Elwany, "A review on process monitoring and control in metal-based additive manufacturing," J. Manuf. Sci. Eng., vol. 136, no. 6, 2014, Art. no. 060801.
- [4] F. Imani, B. Yao, R. Chen, P. K. Rao, and H. Yang, "Fractal pattern recognition of image profiles for manufacturing process monitoring and control," in *Proc. ASME 13th Int. Manuf. Sci. Eng. Conf.*, 2018.
- [5] B. Yao, F. Imani, A. S. Sakpal, E. Reutzel, and H. Yang, "Multifractal analysis of image profiles for the characterization and detection of defects in additive manufacturing," ASME J. Manuf. Sci. Eng., vol. 140, no. 3, 2018, Art. no. 031014.
- [6] Y. Huang, M. C. Leu, J. Mazumder, and A. Donmez, "Additive manufacturing: current state, future potential, gaps and needs, and recommendations," J. Manuf. Sci. Eng., vol. 137, no. 1, 2015, Art. no. 014001.
- [7] Q. Huang, H. Nouri, K. Xu, Y. Chen, S. Sosina, and T. Dasgupta, "Statistical predictive modeling and compensation of geometric deviations of three-dimensional printed products," *J. Manuf. Sci. Eng.*, vol. 136, no. 6, 2014. Art. no. 061008.
- [8] Q. Huang, J. Zhang, A. Sabbaghi, and T. Dasgupta, "Optimal offline compensation of shape shrinkage for three-dimensional printing processes," *IIE Trans.*, vol. 47, no. 5, pp. 431–441, 2015.
- [9] Q. Huang, "An analytical foundation for optimal compensation of threedimensional shape deformation in additive manufacturing," *J. Manuf. Sci. Eng.*, vol. 138, no. 6, 2016, Art. no. 061010.
- [10] E. Savio, L. De Chiffre, and R. Schmitt, "Metrology of freeform shaped parts," CIRP Ann., vol. 56, no. 2, pp. 810–835, 2007.
- [11] D. Dimitrov, K. Schreve, and N. De Beer, "Advances in three dimensional printing-state of the art and future perspectives," *Rapid Prototyping J.*, vol. 12, no. 3, pp. 136–147, 2006.
- [12] F. Imani, A. Gaikwad, M. Montazeri, R. Prahalad, H. Yang, and E. W. Reutzel, "Layerwise in-process quality monitoring in laser powder bed fusion," in *Proc. ASME 2018 13th Int. Manuf. Sci. Eng. Conf.*, 2018.
- [13] H. Krauss, C. Eschey, and M. Zaeh, "Thermography for monitoring the selective laser melting process," in *Proc. Solid Freeform Fabrication Symp.*, 2012, pp. 999–1014.

- [14] E. Rodriguez, J. Mireles, C. A. Terrazas, D. Espalin, M. A. Perez, and R. B. Wicker, "Approximation of absolute surface temperature measurements of powder bed fusion additive manufacturing technology using in situ infrared thermography," Additive Manuf., vol. 5, pp. 31–39, 2015.
- [15] M. Grasso, V. Laguzza, Q. Semeraro, and B. M. Colosimo, "In-process monitoring of selective laser melting: Spatial detection of defects via image data analysis," *J. Manuf. Sci. Eng.*, vol. 139, no. 5, 2017, Art. no. 051001.
- [16] B. Foster, E. Reutzel, A. Nassar, B. Hall, S. Brown, and C. Dickman, "Optical, layerwise monitoring of powder bed fusion," in *Proc. Solid Free. Fabr. Symp.*, 2015, pp. 295–307.
- [17] Z. Du, M. K. Jeong, and S. G. Kong, "Band selection of hyperspectral images for automatic detection of poultry skin tumors," *IEEE Trans. Autom. Sci. Eng.*, vol. 4, no. 3, pp. 332–339, 2007.
- [18] C. Kan and H. Yang, "Dynamic network monitoring and control of in situ image profiles from ultraprecision machining and biomanufacturing processes," Quality Rel. Eng. Int., vol. 33, no. 8, pp. 2003–2022, 2017.
- [19] C. Kan, R. Chen, and H. Yang, "Image-guided quality control of biomanufacturing process," *Procedia CIRP*, vol. 65, pp. 168–174, 2017.
- [20] C. Park, J. Z. Huang, J. X. Ji, and Y. Ding, "Segmentation, inference and classification of partially overlapping nanoparticles," *IEEE Trans. Pattern* Anal. Mach. Intell., vol. 35, no. 3, pp. 1–1, Mar. 2013.
- [21] H. Yan, K. Paynabar, and J. Shi, "Image-based process monitoring using low-rank tensor decomposition," *IEEE Trans. Autom. Sci. Eng.*, vol. 12, no. 1, pp. 216–227, Jan. 2015.
- [22] L. Zhang, K. Wang, and N. Chen, "Monitoring wafers geometric quality using an additive gaussian process model," *IIE Trans.*, vol. 48, no. 1, pp. 1–15, 2016.
- [23] M. Khanzadeh, S. Chowdhury, M. A. Tschopp, H. R. Doude, M. Marufuzzaman, and L. Bian, "In-situ monitoring of melt pool images for porosity prediction in directed energy deposition processes," *IISE Trans.*, pp. 1–19, 2018.
- [24] E. W. Reutzel and A. R. Nassar, "A survey of sensing and control systems for machine and process monitoring of directed-energy, metal-based additive manufacturing," *Rapid Prototyping J.*, vol. 21, no. 2, pp. 159–167, 2015
- [25] A. H. Elwany, N. Z. Gebraeel, and L. M. Maillart, "Structured replacement policies for components with complex degradation processes and dedicated sensors," *Oper. Res.*, vol. 59, no. 3, pp. 684–695, 2011.
- [26] O. Alagoz, H. Hsu, A. J. Schaefer, and M. S. Roberts, "Markov decision processes: A tool for sequential decision making under uncertainty," *Med. Decision Making*, vol. 30, no. 4, pp. 474–483, 2010.